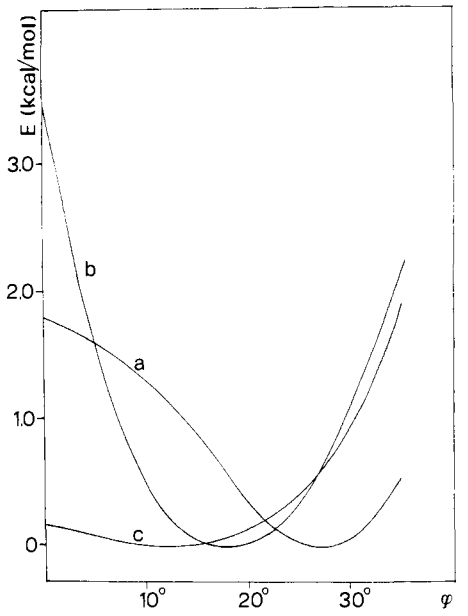

Figure 3. INDO potential energies computed as a function of the angle φ between the $C_1C_2C_3$ plane and the C_2–X bond in the silyl adducts of (a) camphor and (b) thiocamphor and (c) in the camphyl radical.

or S–M bonds which are not symmetrical with respect to the $C_1C_2C_3C_4$ plane. In fact if the C_2–X bond is tilted toward the exo side, the a^H(3-exo) – a^H(3-endo) difference tends to vanish.

In conclusion, the experimental and computed results reported here have shown various interesting points that can be summarized as follows. (i) The radical-center carbon atom in bicyclo-[2.2.1]hept-2-yls and related radicals shows only a slight tendency to adopt a pyramidal geometry as the result of the straining of the $C_1C_2C_3$ bond angle. (ii) The degree of pyramidalization, which is expected to be quite small for X = H, can be considerably larger when electronegative substituents X, having a π-type lone pair, are attached to C_2. First-row heteroatoms cause a greater pyramidalization than second-row heteroatoms, in agreement with theoretical predictions.[13] (iii) Estimates of the tilt angle based on the difference between the 3-exo and 3-endo proton couplings may be misleading, since these splittings are predicted to be inequivalent even for a planar configuration at C_2. Moreover, distortions of the carbon skeleton resulting in a twisting of the molecule around the C_1C_4 axis may further increase this inequivalence.[4]

Experimental Section

The transient metal-centered radicals were generated within the cavity of the ESR spectrometer by room temperature photolysis, with a high pressure mercury lamp, of degassed solutions of the carbonylic or thiocarbonylic substrate in *tert*-butylbenzene containing the appropriate triaryl or trialkyl metal hydride and di-*tert*-butyl peroxide.[14] With camphor only the silyl adduct could be observed in these conditions. While thiocamphor was prepared according to well-established methods, all other chemicals were commercially available and were used without further purification.

Acknowledgment. Financial support from C.N.R. (Rome) is gratefully acknowledged by G.F.P.

(12) Inagaki, S.; Fujimoto, H.; Fukui, K. *J. Am. Chem. Soc.* **1976**, *98*, 4054.

(13) Bernardi, F.; Epiotis, N. D.; Cherry, W.; Schlegel, H. B.; Whangbo, M. H.; Wolfe, S. *J. Am. Chem. Soc.* **1976**, *98*, 469.

(14) Alberti, A.; Guerra, M.; Pedulli, G. F. *J. Chem. Soc., Perkin Trans. 2* **1979**, 1568.

Threshold Intensities and Kinetics of Sonoreaction of Thymine in Aqueous Solutions at Low Ultrasonic Intensities

Chandra M. Sehgal and Shih Yi Wang*

Contribution from the Division of Environmental Chemistry, The Johns Hopkins University, COEH-U.S.P.H.S. Hospital, 3100 Wyman Park Drive, Building 6, Baltimore, Maryland 21211.
Received March 9, 1981

Abstract: In this study, the threshold intensities and kinetics of sonoreaction of thymine in aqueous solutions are investigated under different experimental conditions. The results show that in the limiting case of zero aeration rate the threshold for thymine reaction is 1.7 W/cm^2. The experiments were carried out under a controlled and well-defined acoustic field and the influence of various important factors (spatial average acoustic intensity, bubbling rate, solution temperature kinetics) has been investigated. Tentative theories of cavitation and the accompanying chemical processes are proposed on the basis of experimental results. At relatively higher acoustic intensities (>3 W/cm^2) the cavitation chemistry of thymine is significantly reduced. This has been attributed largely to the change in the number of cavitating bubbles due to an increasing degree of coalescence. The results also suggest that the sonoreaction may take place in the bubble–liquid interphase and the reaction kinetics change with the solution temperature. This is due to converse changes in cavitation intensity and thymine diffusion as the solution temperature is altered.

Nucleic acid components, under a variety of experimental conditions, are known to undergo sonoreaction in an ultrasonic field.[1-5] These studies largely deal with the production, isolation, and identification of sonoproducts. In order to understand ultrasonic toxicity at a molecular level, it is necessary to investigate the reaction kinetics, the threshold intensities for the reactions of nucleic acid components, and how the threshold intensities change with cavitation conditions, viz., bubbling activity, solution temperature, etc.

(1) McKee, J. R.; Christman, C. L.; O'Brien, W. D., Jr.; Wang, S. Y. *Biochemistry* **1977**, *16*, 4651.

(2) Gupta, A. B.; Wang, S. Y. *Ultrasonic Symp. Proc., IEEE* **1976**, *No. 76 CH1120-5SU*, 92–6.

(3) Mead, E. L.; Sutherland, R. G.; Verrall, R. E. *Can. J. Chem.* **1975**, *53*, 2394.

(4) Craig, W., Ph.D. Thesis, University of Saskatchewan, Canada, 1979.

(5) El'piner, I. E. "Ultrasound: Physical, Chemical and Biological Effects"; Consultant Bureau: New York, 1964; p 53.

0002-7863/81/1503-6606$01.25/0

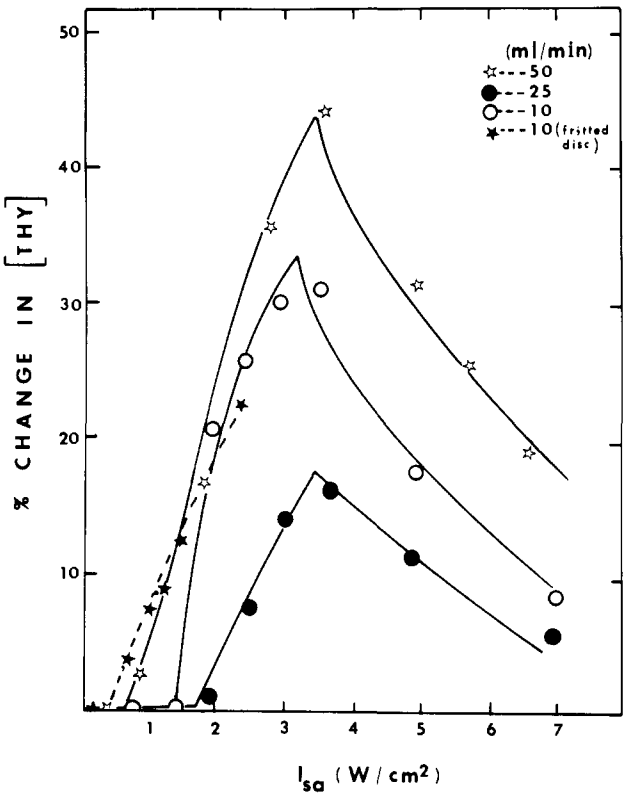

Figure 1. Sonoreaction of thymine as a function of spatial average ultrasonic intensity (I_{sa}), temperature 37.5 °C.

The earlier results on the sonoreaction kinetics of nucleic acid components,[1,3] the temperature dependence of corrosion,[6] chemical activity,[7] and sonoluminescence[8] have been conflicting. Therefore, with use of thymine (Thy) as a model compound, a systematic investigation of its sonoreaction as a function of acoustic intensity (1–7 W/cm²), solution temperatures (20–70 °C), and sonication time was carried out. The findings are explained in terms of inter- and intrabubble interactions and a diffusion model which is similar to that proposed to explain the chemical reactions in the early stages of radiolysis[9] and sonolysis[10–13] of water.

Experimental Section

The ultrasonic apparatus and procedures have been described in detail.[1,14,15] All the results reported here are in terms of the continuous wave spatial average ultrasonic intensity (I_{sa}) with a spatial peak intensity to I_{sa} ratio of 1.4. The irradiations were carried out at a frequency of 0.99 ± 0.01 MHz.

Aliquots (15 mL) of 0.1 mM Thy solutions were filled in the sonication cell and individually suspended vertically in the irradiation tank maintained at a known temperature on the X axis and in the far field of ultrasonic beam. The solution was preaerated at a known rate for 10 min while it thermally equilibrated with the bulk solution. The bubbling rate was monitored by a pressure gauge and a flowmeter. The sonochemical reaction of Thy was determined from the UV absorption of the solution in the region 200–360 nm, using a Beckman DU-8 recording spectrophotometer.

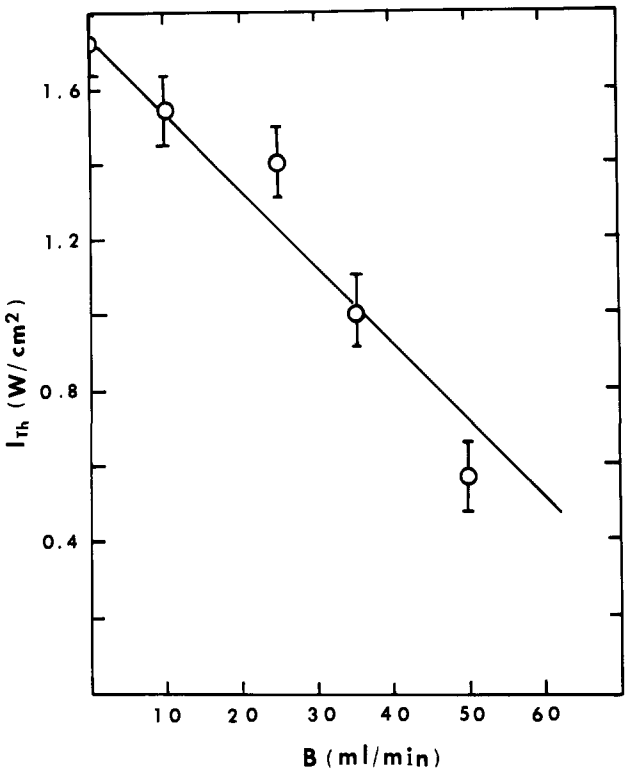

Figure 2. Dependence of threshold intensity (I_{Th}) of sonoreaction on the bubbling rate (B), temperature 37.5 °C.

Results and Discussion

Effect of Ultrasonic Intensity on the Sonoreaction of Thy. Oxygen saturated aqueous solutions of Thy were sonicated for 30 min at different I_{sa} at a known bubbling rate. The results (Figure 1) show that sonoreaction of Thy does not occur until a threshold value of ultrasonic intensity I_{Th} is exceeded. A further increase in ultrasonic intensity increases the sonoreaction until a maximum is reached after which the sonoreaction diminishes with a tailing of the curve at high intensities.

The curves of Figure 1 also show that the threshold intensity increases with a decrease in the bubbling rate [B] during sonolysis. A plot in Figure 2 of I_{Th} vs. [B] shows a linear relationship between the two variables. In the limiting case of zero bubbling rate the I_{Th} is 1.7 W/cm². For a fixed bubbling rate (e.g., 10 mL/min) when sintered glass was used, there was a decrease in I_{Th} as shown by the dotted lines in Figure 1. Because the solutions were saturated with a gas prior to sonication by preaeration, and because the sonoreaction increases with the bubbling rate, it follows that cavitation activity depends directly upon the "undissolved" component of the gas, as suggested earlier.[8,16] Evidently, the increased bubbling activity, either by increasing the bubbling rate or by using a fritted disk, increases the "undissolved" gas content in the liquid. This induces a drop in the tensile strength[17] of the liquid and, consequently, reduces I_{Th}.

Returning to the question of the shape of chemical activity vs. acoustic intensity curves of Figure 1, it is observed that the published curves may be classified into two categories: those that have a maximum at an optimum intensity[18,19] (Figure 1) and those that increase linearly with intensity.[20–24] Such a dependence of

(6) Ibisi, M.; Brown, B. *J. Acoust. Soc. Am.* **1967**, *41*, 568.
(7) Rosenberg, L. D. *Ultrasonic News*, **1960**, *4*, 16.
(8) Sehgal, C.; Sutherland, R. G.; Verrall, R. E. *J. Phys. Chem.* **1980**, *84*, 525.
(9) Draganic, I. G.; Draganic, Z. D. "The Radiation Chemistry of Water"; Academic Press: New York, 1970; p 123.
(10) Margulis, M. A., *Russ. J. Phys. Chem.* (*Engl. Transl.*) **1976**, *50*, 534.
(11) Margulis, M. A., *Dokl. Akad. Nauk. SSSR*, **1974**, *218*, 616.
(12) Margulis, M. A. *Sov. Phys.-Acoust.* (*Engl. Transl.*) **1976**, *21*, 356.
(13) Margulis, M. A. *Sov. Phys.-Acoust.* (*Engl. Trans.*) **1976**, *21*, 468.
(14) O'Brien, W. D., Jr.; Christman, C. L.; Yarrow, S. *Ultrasonic Symp., Proc. IEEE* **1974**, *No. 74 CHO 896 13U*, 57.
(15) Hattman, T., Thesis, School of Hygiene and Public Health, The Johns Hopkins University, Baltimore, Maryland, 1976.
(16) Knapp, R. J.; Daily, J. W.; Hammit, F. G. "Cavitation"; McGraw-Hill: New York, 1972; p 62.
(17) Il'Chev, V. I. *Sov. Phys. Acoust.* (*Engl. Transl.*) **1967**, *13*, 259.
(18) Hill, C. R. *J. Acoust. Soc. Am.* **1972**, *52*, 667.
(19) Weissler, A. *J. Acoust. Soc. Am.* **1953**, *25*, 651.
(20) Griffing, V.; Sette, D. *J. Chem. Phys.* **1955**, *23*, 503.
(21) Lindström, O. *J. Acoust. Soc. Am.* **1955**, *27*, 654.
(22) Miller, N. *Trans. Faraday Soc.* **1950**, *46*, 546.
(23) Bunsel, R.; Picard, D.; Bouzignes, H. *J. Chim. Phys. Phys.-Chim. Biol.* **1953**, *50*, 97.

chemical yields on sonic intensity has been explained differently by various researchers, and a unified view or a general theory to explain both kinds of curves is lacking. There is growing evidence[25-32] that bubbles disintegrate to generate microbubbles, while at the same time the constantly changing pressure gradient of the ultrasonic field, stirring of the solution, Bjerknes forces, and surface waves cause the bubbles to come close together and coalesce. The mechanism by which fragmentation occurs is not clearly understood. One possibility is that near the end of a compression cycle the intracavity gas–vapor mixture reaches a highly compressed state and behaves as a liquid of low compressibility. The convolution of surface waves at the interface, the intense inward force of the converging walls, and the incapability of the cavity contents for further compression generates strain at the bubble surface. This would initially deform the spherical bubble and eventually rupture its surface. The cavity contents fly apart as small fragments called microbubbles. These bubbles, in turn, may act as nuclei for cavitation.

At low-pressure amplitudes, the collapse time, τ, is small compared to the time period of ultrasound, $\bar{T}$, and the bubbles undergo a complete collapse before the end of the pressure cycle. Almost all the nuclei that grow into bubbles undergo cavitation. The net process can be schematically represented as:

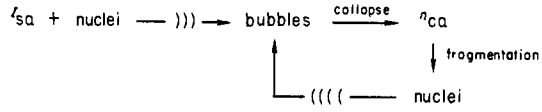

where n_{ca} is the number of bubbles that cavitate, N is the number of bubbles that grow to a maximum radius and, χ is the number of gas nuclei present in the liquid medium. As N is directly related to the pressure amplitude (i.e., $I_{sa}^{1/2}$) an increase in it induces an increase in n_{ca} and the chemical activity associated with them. This continues until pressure amplitude reaches a value at which the collapse times of the cavitating bubbles become comparable to or exceed $\bar{T}/2$ (i.e., $\tau \gtrsim \bar{T}/2$). Under such circumstances the collapse of bubbles is not complete before the end of the positive phase of the ultrasonic cycle.[25b] The inward motion of a bubble on its way to collapse is arrested by the negative phase of the pressure cycle. Consequently, the bubble does not collapse in every acoustic period but instead it oscillates a few times before collapsing. This is in agreement with the theoretical studies based on numerical analysis of Noltingk and Neppiras's equation defining the dynamics of bubbles.[33] The increased time interval between the birth and collapse gives oscillating bubbles greater opportunity to interact among themselves according to Bjerknes forces. When the oscillating bubbles oscillate in phase, a negative force (implying attraction) arises between the interacting bubbles (see eq 11, ref 31) and they coalesce before collapsing. This effect may further be enhanced in a complex fashion by the second-order effect of the bubbles interfering with each other's radiation field.[34] Because each vibrating bubble generates a scattered wave, the total driving force seen by a given bubble is the algebraic sum of the ambient sinusoidal pressure field of ultrasound and the field scattered by all the neighboring bubbles. Although the second-order effect of the bubbles interfering with each other's radiation field could be important, it is not yet possible to determine its influence on cavitation quantitatively. Under such conditions of enhanced coalescence the net process can be schematically represented as:

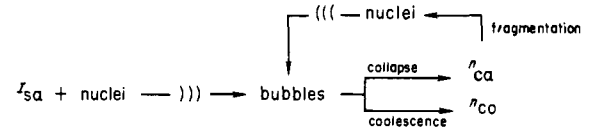

Due to coalescence the number of bubbles that undergo cavitation is reduced. This, further, decreases the number of microbubbles formed by fragmentation and, consequently, N. Along with all of this, the larger collapse times diminish the adiabaticity of bubble collapse and make cavitation less efficient. Thus, in conclusion, the intensity of collapse as well as the number of bubbles that undergo cavitation decrease after a certain pressure amplitude is reached. As a result of this, the chemical activity vs. the ultrasonic intensity curves show a decrease after reaching an optimum value.

If the experimental conditions are such that bubble interactions are negligibly small, the cavitation-induced effects increase linearly with ultrasonic intensity as observed experimentally.[20,22,23] With an increase in bubble interactions, coalescence plays a more significant role and the curve loses linearity as observed experimentally by Lindström.[21] Finally, under the experimental conditions of strong bubble interactions, the chemical activity induced by cavitation decreases after an optimum intensity as observed in the present experiments and by the previous researchers.[18,19]

Temperature Dependence of Sonoreaction. The sonoreaction of Thy was measured at different temperatures by sonicating the solution for 20 min. The results show (Figure 3) that as the temperature of the solution is increased the sonoreaction increases initially and then levels off to a horizontal plateau. A further increase in temperature diminishes the rate of sonoreaction.

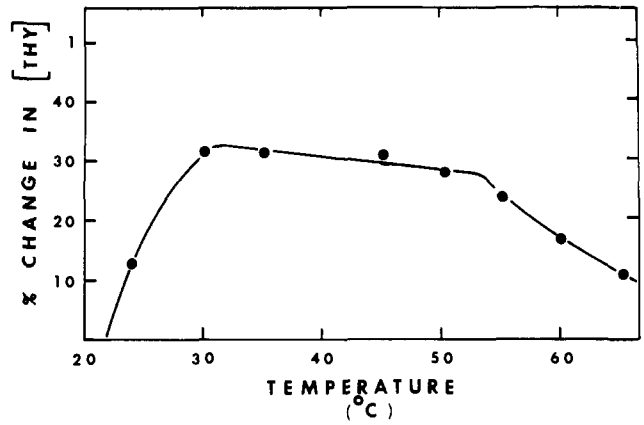

Figure 3. Sonoreaction of thymine at different solution temperatures.

At this time, the results on the chemical and physical activity of cavitation as a function of solution temperature can be grouped into three categories: those that are initially independent of temperature range and then decrease rapidly;[19,21] those that decrease exponentially;[7,8] and finally, those that increase initially after an optimum temperature decrease.[6] These different observations are believed to be due to the phase in which the reaction leading to chemical degradation occurs (i.e., whether it occurs in the liquid medium or in the gaseous phase within a cavity or at a liquid-gas interphase) and to the physical and chemical properties of the medium (e.g., concentration of the solute).

In order to understand this problem, consider a spherical cavity (Figure 4) in the final stages of collapse. The cavity is surrounded by an infinite mass of water at a constant temperature. The volume between the two spheres in Figure 4 represents the interphase.[35]

(24) Sirotyuk, M. G. *Akust. Zh.* **1964**, *10*, 465.
(25) (a) Rosenberg, L. D. "High Intensity Ultrasonic Fields"; Plenum Press: New York, 1971; Chapter 3; (b) *Ibid.*, Chapter 2.
(26) Willard, G. W. *J. Acoust. Soc. Am.* **1954**, *26*, 9333A.
(27) Hawkins, S. D. *J. Acoust. Soc. Am.* **1966**, *39*, 55.
(28) Temple, P.; Detenbeck, R. W.; Nyborg, W. L. *J. Acoust. Soc. Am.* **1971**, *50*, 112A.
(29) Neppiras, E. A.; File, E. E. *J. Acoust. Soc. Am.* **1969**, *46*, 1264.
(30) Nyborg, W. L.; Rodgers, A. *Biotechnol. Bioeng.* **1967**, *9*, 235.
(31) Crum, L. S. *J. Acoust. Soc. Am.* **1975**, *57*, 1963.
(32) Saxena, T. K.; Nyborg, W. L. *J. Chem. Phys.* **1970**, *53*, 149.
(33) Akuliche, V. A. *Sov. Phys.–Acoust. (Engl. Transl.)* **1967**, *13*, 149.
(34) Coakley, W. T.; Nyborg, W. L. "Ultrasound: Its Application in Medicine and Biology"; Elsevier Scientific Publishing Co.: New York, 1978; Part 1, p 119.

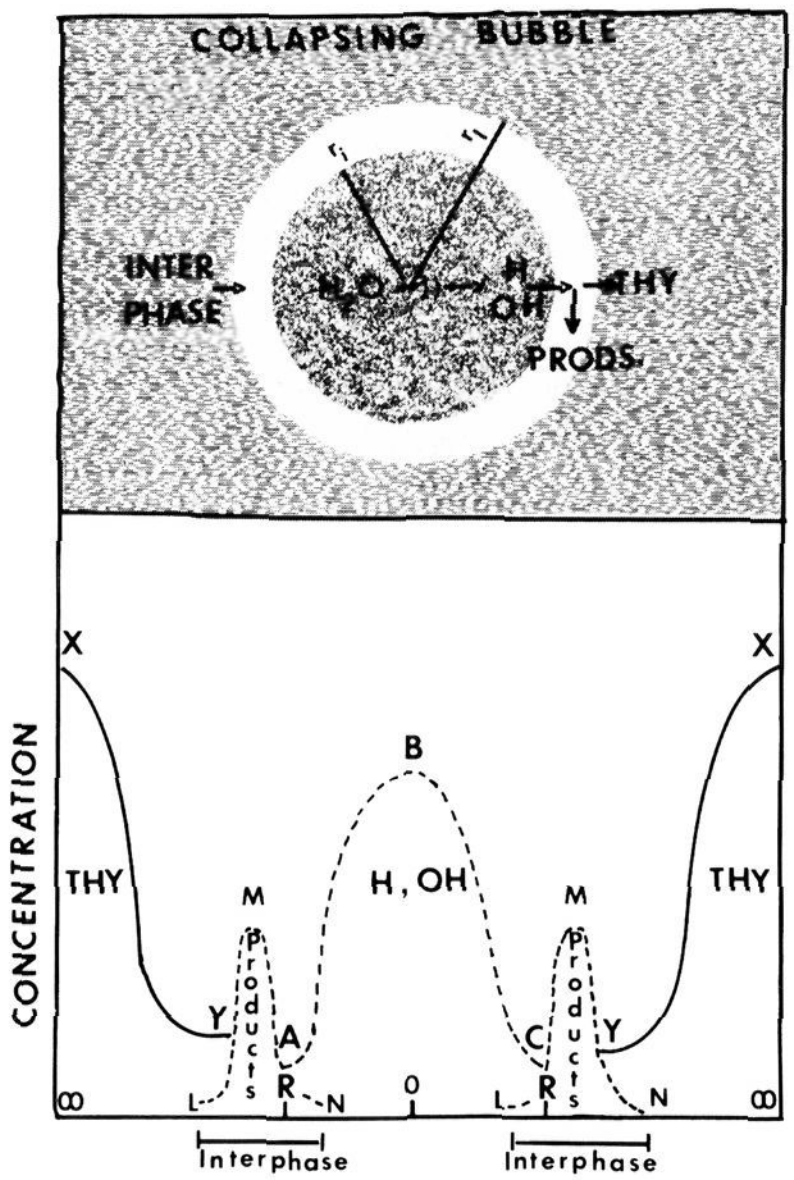

Figure 4. Schematics of the diffusion model.

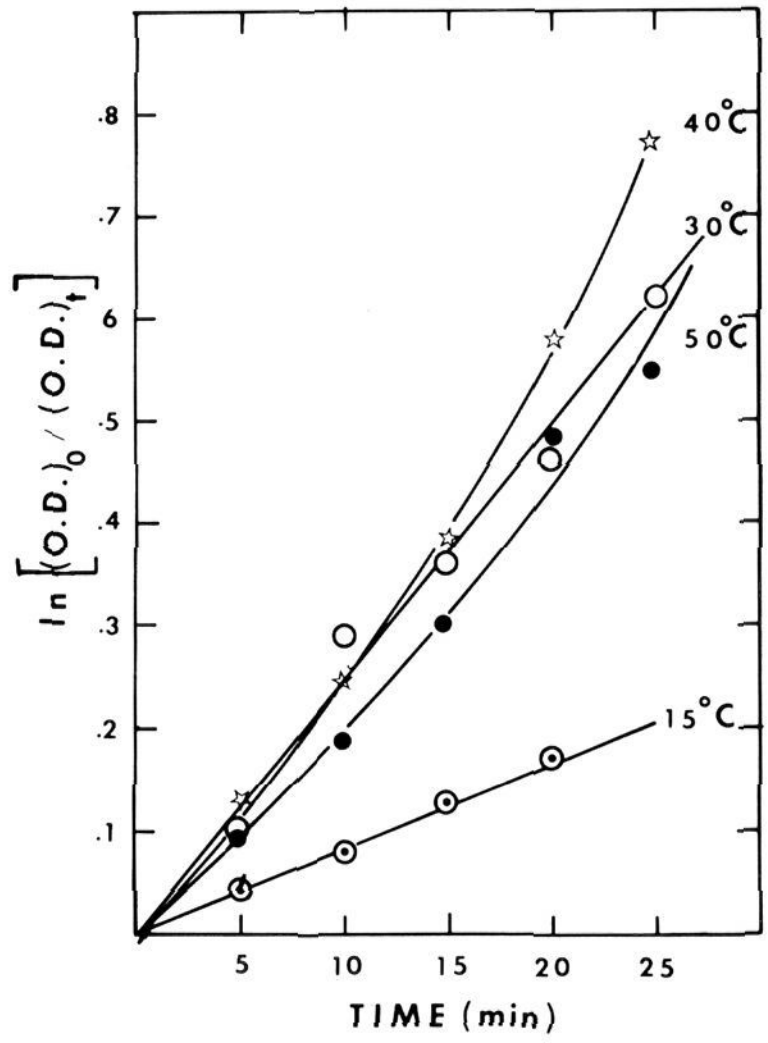

Figure 5. First-order plots of the sonoreaction of thymine at various temperatures.

As the bulk solution temperature is raised, the vapor pressure of the liquid increases. The increased vapor content inside the cavities increases the cushioning action[36] during the compression, weakens the collapse, and reduces the cavitation intensity. Thus, any effect directly related to cavitation (e.g., sonoluminescence) should correspondingly decrease with an increasing temperature. Any variation from the above as observed in the present and some prior studies[6,19,21] suggests that the sonoreaction of nonvolatile substances (e.g., Thy) with the free radicals (generated inside the cavities) does not occur appreciably inside the cavity. More likely, it occurs in the bubble–liquid interphase.

The bottom of Figure 4 shows a qualitative distribution of concentrations of Thy, free radicals, and the sonoproducts in the vicinity of a collapsing bubble near the end of compression. The concentration of free radicals is maximum at the center of the bubble, and decreases according to a Gaussian function[11] as one approaches the interphase due to its reaction with free radicals (curve ABC, Figure 4).

The concentration and temperature gradients inside a bubble and in the solution force the free radicals and Thy to diffuse into the interphase from opposing directions. In the interphase, which acts as the reaction zone, these chemical species react almost instantaneously (rate constants $\sim 10^9$ M^{-1} s^{-1}),[37,38] and there is a buildup of concentration of the sonoproduct which may also be represented by a Gaussian curve with a maximum at the center of the interphase (curve LMN, Figure 4).

At a relatively low temperature, the cavitation is intense and there is an abundance of free radicals which rapidly diffuse into the interphase. On the other hand, the diffusion of Thy into the interphase is slow and it is, therefore, the rate-determining step. As the temperature of the solution is raised, a greater amount of Thy diffuses into the interphase, and an increase in the sonoreaction occurs (see below).

At the intermediate stage, the two rates of diffusion become comparable. In this temperature range, the increase in sonoreaction by acceleration in diffusion of Thy is neutralized by a reduction in the diffusion of free radicals. Therefore, there will be no net change in the sonoreaction, and a plot of percent sonoreaction vs. temperature curve will be horizontal, as observed experimentally (Figure 3).

A further rise in solution temperature would inhibit cavitation to such an extent that the diffusion of free radicals would become the rate-determining step. This would decrease sonoreaction as the solution temperature is raised. (Figure 3).

It appears that the chemical activity vs. temperature curves observed by Weissler and Lindström are parts of a general curve of the type shown in Figure 3. The breaks in the curve[19,21] occur at different temperatures due to a difference in the substrate concentrations, diffusion coefficients, and different cavitation conditions.

Kinetics of Sonoreaction of Thymine. From the previous section, it follows that a change in the rate-determining step with the solution temperature should change the kinetics of the reaction. This was verified by a kinetics study, and the results are shown in Figure 5. Plots of ln $[(OD)_0/(OD)_t]$ are linear at 15 and 30 °C; i.e., the reaction is of the first order. The curves deviate from linearity at 40 and 50 °C, thereby indicating a change in the order of reaction. A plot of OD vs. time at 50 °C is linear, indicating the reaction to be of zero order (Figure 6).

The variation of reaction order with temperature can be explained with the help of a cavitation–diffusion model proposed by Margulis.[10–13] Degradation of Thy with ultrasound leads to the formation of cis and trans glycols[1–3] along with several other

(35) As mentioned earlier, near the end of the compression stage, the gas–vapor mixture in the cavity is in a highly compressed state; i.e., there may not be a well-defined physical boundary. However, due to the different chemical compositions of the gas–vapor mixture, its behavior will be very different from the surrounding liquid. Therefore, an interphase in this situation is defined as a zone whose chemical properties are intermediate between the cavity contents and the surrounding liquid.

(36) The term "cushioning action" refers to the resistance offered by the cavity contents to the inward motion of a bubble during its collapse. Because the cavity contents reach a super-critical state during compression, this resistance is offered by both gas as well as vapor contained inside a cavity.

(37) Schole, G. "Photochemistry and Photobiology of Nucleic Acids"; Wang, S. Y., Ed.; Academic Press: New York, 1976; Vol. 1, Chapter 12.

(38) Spinks, J. W. T.; Woods, R. J. "An Introduction to Radiation Chemistry"; J. Wiley and Sons: New York, 1976.

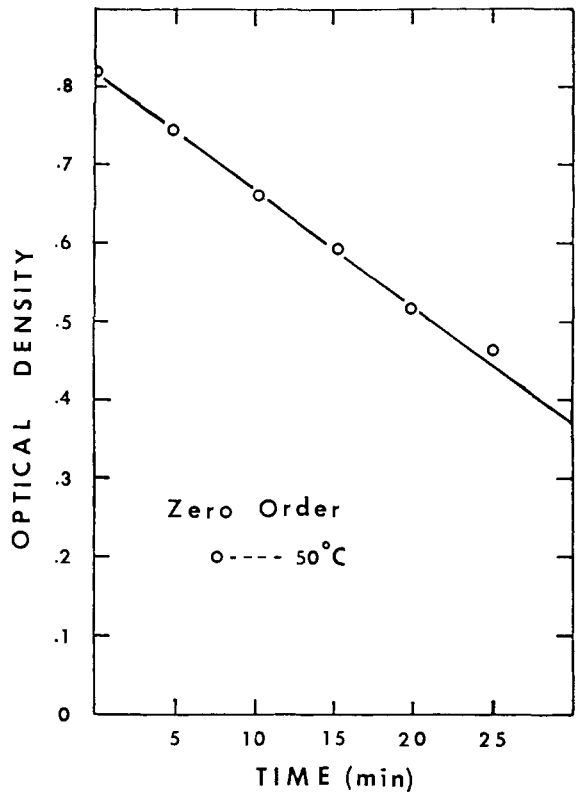

Figure 6. Zero-order kinetics of the sonoreaction of thymine at 50 °C.

products.[3] During cavitation, the decomposition of water produces H· and ·OH radicals. In the presence of O_2, the hydrogen radicals rapidly combine with O_2 to form HO_2·. The initial step of sonolysis under these conditions is the addition of hydroxyl radicals across the 5–6 double bond of Thy. The thymine radicals so formed react instantaneously with HO_2· to give adducts which subsequently degrade in several ways to give the final products.[3]

The differential equation describing the dependence of radical concentration, C, on time, t, and distance, r, from the center of an isolated, spherically symmetrical bubble for a single-radical model can be written in the form[12]

$$\frac{dC}{dt} = D\frac{\delta^2 C}{\delta r^2} + \frac{2D}{r}\frac{\delta C}{\delta r} + Dk_t\frac{\delta^2 \ln T}{\delta r^2} + \frac{2Dk_t}{r}\frac{\delta \ln T}{\delta r} - kC^2 - k'CS \quad (1)$$

where D is the diffusion coefficient, k_t is the thermal diffusion ratio, T is the intracavity temperature, and k and k' are the rate constants for the recombination of radicals and their reaction with Thy of concentration S, respectively.

Thermal diffusion takes place in the time interval $t < 10^{-9}$–10^{-11} s.[12] For $t > 10^{-8}$ s, only concentration diffusion and chemical reactions are observed and eq 1 simplifies to the form[12]

$$\frac{dC}{dt} = D\frac{\delta^2 C}{\delta r^2} + \frac{2D}{r}\frac{\delta C}{\delta r} - kC^2 - k'CS \quad (2)$$

By similar reasoning, the space–time distribution of the substrate concentration, S, is shown by the equation[12]

$$\frac{dS}{dt} = D_s\frac{\delta^2 S}{\delta r^2} + \frac{2D_s}{r}\frac{\delta S}{\delta r} - k'CS \quad (3)$$

where D_s is the diffusion constant for Thy.

Since the chemical reactions in the interphase involve several consecutive steps, the net rate observed for the degradation of Thy will be determined by the slowest single step. The radical–radical recombination and radical–thymine reactions occur almost instantaneously. Therefore, the degradation rate will be controlled by the relative rates of diffusion of free radicals and/or Thy into the interphase.

Case I. At low solution temperatures, the cavitation activity is intense. Due to relatively high intracavity temperatures and radical concentrations, the radicals will rapidly diffuse into the interphase. Under such circumstances, the diffusion of Thy into the interphase will be the rate-determining step; that is, Thy will be used up as soon as it diffuses into the reaction zone. Consequently, the boundary conditions at the outer boundary of the interphase of radius, r_1, will be

$$S(I,t) \rightarrow 0 \quad (4)$$

$$dS/dr \rightarrow [\text{Thy}] - S = [\text{Thy}] \quad (5)$$

$$d^2S/dr^2 \rightarrow 0 \quad (6)$$

and

$$-d[\text{Thy}]/dt \propto \frac{dS}{dt} = (2D_s/r_1)[\text{Thy}] \quad (7)$$

Therefore at low solution temperatures, the thymine degradation is of first order, as observed experimentally.

The number of moles of Thy, ΔS, passing into the interphase of the surface, $4\pi r_1^2$, during the collapse time, τ, of the bubble can be shown by the expression

$$\Delta S \simeq 8\pi D_s r_1 \tau[\text{Thy}] \quad (8)$$

As the solution temperature is increased, the diffusion coefficient as well as the intracavity chemical composition changes. The change in cavity composition alters the dynamics of the bubbles, thereby affecting r_1 and τ. It is not yet feasible to quantitatively correlate ΔS (proportional to percent degradation at low solution temperatures) to D_s, r_1, and τ because it is not yet possible to measure D_s or chemical composition of a bubble as a function of solution temperature under cavitation conditions. However, to a first approximation it may be argued that an increase in solution temperature would increase the vapor content of cavitation bubbles and, therefore, reduce the intensity of collapse. This would imply greater values of r_1 and τ for the cavitation bubbles. This can be further illustrated in the following way:

The minimum radius, r_{min}, of the cavitation bubble containing the gas–vapor mixture is related to vapor pressure, P^0_v, by the expression[39a]

$$r_{min} \cong 3r_{max}(\chi_g P^0_g + \chi_v P^0_v)/P_H \quad (9)$$

where χ_g and χ_v are the mole fractions of gas and vapor contents, respectively, P^0_g is the vapor pressure of pure gas, r_{max} is the radius at which collapse begins, and P_H is the hydrostatic pressure. As the solution temperature is raised, r_{max},[39b] χ_v and P_v increase, thereby increasing the r_{min}, and the radius of interphase associated with it, i.e., r_1.

The collapse time of the Rayleigh type cavity containing vapor can be shown by the following expression:[40]

$$\tau \cong 0.915[\rho/(P_H - P_v)]^{1/2} r_{max} \quad (10)$$

Once again, an increase in temperature would lead to an increase in τ. Also, under the turbulent conditions caused by shock waves and microstreaming near a rapidly collapsing bubble, the diffusion coefficient may be expected to change significantly with solution temperature. The increase in D_s, τ, and r_1 with solution temperature would increase ΔS and, consequently, percent degradation of Thy as observed experimentally (Figure 3).

Case II. In the limiting case of high solution temperatures, the cavitation intensity is significantly reduced. This leads to lower intracavity temperature and free-radical concentrations. As a result of this, the diffusion of free radicals into the reaction zone is greatly reduced and, consequently, it becomes the rate-deter-

(39) (a) Sirotyuk, M. D. "High Intensity Ultrasonic Field"; Rozenberg, L. D., Ed.; Plenum Press: New York, 1971; p 300; (b) Ibid., p 330.
(40) Plesset, M. D.; Prosperetti, A. *Annu. Rev. Fluid Mech.* **1977**, *9*, 145.

mining step. The same situation may occur at high concentration of Thy. Under these circumstances, the radicals will be used up as soon as they diffuse into the interphase, and the boundary conditions at the inner boundary of the interphase of radius, r_i, will be

$$C(i,t) \rightarrow 0 \tag{11}$$

$$-\frac{d[Thy]}{dt} \propto \frac{dC}{dt} = D\frac{\delta^2 C}{\delta r^2} + \frac{2D}{r_i}\frac{\delta C}{\delta r} \tag{12}$$

That is, the reaction is of zero order with respect to Thy at high solution temperatures and thymine concentrations. The experiments reported by Mead et al.[3] were carried out at high concentration of Thy (10 mM), and the reaction was found to be zero order. On the other hand, the results reported by McKee et al.[1] were carried out at low uracil concentration (0.1 mM) and the reaction order was found to be unity. Therefore, the results of previous studies[1,3] as well as the present results can be explained as specific cases of a general theory proposed here.

At high solution temperatures, the number of moles, ΔC, of radicals that diffuse into the interphase during the collapse time of the bubble will be given by the expression

$$\Delta C \simeq 8\pi D r_i \tau C_i \tag{13}$$

where C_i is the radical concentration at the bubble surface. Due to a sharp decrease in intracavity temperature as the solution temperature is raised, D and C_i will be significantly reduced. Therefore, even though r_i and τ will increase, with an increase in solution temperature, the number of moles of free radicals that diffuse into the interphase will be greatly reduced leading to a lower degree of degradation of Thy as shown in Figure 3.

Case III. At moderate temperatures, wherre the two diffusion rates are comparable, the net rate of degradation of Thy will be the sum of the two rates of diffusion, i.e.,

$$-\frac{d[Thy]}{dt} = D\frac{\delta^2 C}{\delta r^2} + \frac{2D}{r_i}\frac{\delta C}{\delta r} + D_s\frac{\delta^2 S}{\delta r^2} + \frac{2D_s}{r_1}\frac{\delta S}{\delta r} \tag{14}$$

In this case, the reaction kinetics will be complex with reaction order between the two limiting cases, i.e., 0 and 1.

Conclusions

The present studies show that there is a change in kinetics of the reaction of Thy with a change in the temperature of the solution. Also, at spatial average ultrasonic intensities as low as 1.7 W/cm^2 there is a detectable chemical change. At an aeration rate of 50 mL/min and 34 °C the concentration of thymine is reduced to half in 30 min. This means an average 3×10^{-8} mol or 1.8×10^{16} molecules of Thy reacted per second per liter. The chemical rate is large enough to produce a substantial chemical change during prolonged sonication of living systems.

Acknowledgment. This work was supported by grants from the Food and Drug Administration (RO1 FD00675) and from the National Institute of Environmental Health Sciences (PO1 ES02300). We are also thankful to Drs. W. D. O'Brien, Jr., C. L. Christman, and A. Weissler for their advice and comments.

Reactions of Copper(I) with Micellar Porphyrins and Hemes. Spectroscopic Evidence for Copper(I)–Heme Binuclear Ion Formation

Eugene A. Deardorff, Paulette A. G. Carr, and James K. Hurst*

Contribution from the Department of Chemistry and Biochemical Sciences, Oregon Graduate Center, Beaverton, Oregon 97006. *Received March 2, 1981. Revised Manuscript Received June 29, 1981*

Abstract: Addition of cuprous ion to sodium dodecyl sulfate solubilized porphyrins and ferrihemes containing olefinic substituent groups gives rise to spectral perturbations diagnostic of Cu(I) π complexation. The hemes undergo slow subsequent demetalation in acidic solution, forming porphyrin dications; in the presence of high concentrations of Cu(II) ion the corresponding cupriporphyrins are also formed. For ferriprotoporphyrin IX, the rate of product formation is *inversely* dependent upon the Cu(II) ion concentration; the data are interpreted in terms of a reaction mechanism, the central feature of which is a dynamic equilibrium between oxidized and reduced hemes, i.e., $Fe^{III}PPIX–Cu^{I} + Cu(I) \rightleftarrows Fe^{II}PPIX–Cu^{I} + Cu(II)$. This interpretation is supported by the observation that hemes containing electron-withdrawing substituents in β-pyrrolic positions are extensively reduced to the ferro state by copper(I), but hemes lacking these groups remain primarily ferric when mixed with the cuprous reagent. The reduced Fe(II)–Cu(I) and mixed-valent Fe(III)–Cu(I) binuclear ions are discussed as potential structural models for the oxygen-binding site in cytochrome oxidase.

Cytochrome oxidase is a complex biological particle which acts as the terminal oxidase in mitochondrial respiratory chains. It contains at least seven different protein subunits and associated phospholipids, as well as two distinct heme and copper metal centers, each of which is generally thought to function as a redox carrier in physiological reactions.[1,2] The molecular organization of cytochrome oxidase is presently poorly understood, precisely because of its great structural and dynamic complexity. One conceptual model which is capable of accounting for a wide range of spectroscopic and magnetic data is based upon the hypothesis that the oxygen reduction site is an antiferromagnetically coupled heme *a*–copper(II) binuclear ion.[3] This proposal has stimulated

(1) For recent reviews, see: Wilson, D. F.; Erecinska, M. *Porphyrins* **1980**, *7*, 1–51. King, T. E.; Orii, Y.; Chance, B.; Okunuki, K. "Cytochrome Oxidase"; Elsevier: Amsterdam, 1979. Caughey, W. S.; Wallace, W. J.; Volpe, J. A.; Yoshikawa, S. *Enzymes* **1976**, *13*, 299–344; Wharton, D. C. In "Inorganic Biochemistry"; Eichhorn, G. I., Ed.; Elsevier: Amsterdam, 1973; Vol. 2, pp 955–987.

(2) An alternative view has been presented (Selter, C. H. A.; Angelos, S. G. *Proc. Natl. Acad. Sci. U.S.A.* **1980**, *77*, 1806–1808) in which it is proposed that one of the copper sites remains univalent during oxygen reduction, the cytochrome a_3 site acting as a two-electron donor.

(3) Palmer, G.; Babcock, G. T.; Vickery, L. E. *Proc. Natl. Acad. Sci. U.S.A.* **1976**, *73*, 2206–2210 and references therein.

0002-7863/81/1503-6611$01.25/0